ORIGINAL PAPER

Rasa Pauliukaite · Monica Florescu
Christopher M. A. Brett

Characterization of cobalt- and copper hexacyanoferrate-modified carbon film electrodes for redox-mediated biosensors

Abstract Cobalt and copper hexacyanoferrate films (CoHCF and CuHCF) were formed at carbon film electrodes by three different one-step processes: cycling the applied potential, application of a constant current, and chemically. All hexacyanoferrate films obtained were characterized electrochemically by cyclic voltammetry and electrochemical impedance spectroscopy. To evaluate their possible use as redox mediators for biosensors, they were applied to the determination of hydrogen peroxide in neutral phosphate buffer saline electrolyte. Chemically deposited CuHCF was found to be generally the most suitable as a mediator, although CoHCF made by potential cycling is the most useful when a very low detection limit is necessary.

Keywords Cobalt hexacyanoferrate · Copper hexacyanoferrate · Carbon film electrode · Electrochemical impedance spectroscopy · Hydrogen peroxide determination

Introduction

Transition metal cyanide complexes have been attractive subjects of study for several centuries in different fields of chemistry and physics [1]. The first transition metal cyanide coordination compound obtained was iron(III) hexacyanoferrate(II) or Prussian Blue (PB), which has had broad applications up until now, owing to its favourable properties as a pigment [1–3]. Recently, various other transition metal hexacyanoferrates have been synthesized chemically and electrochemically and characterized by spectroscopic and electrochemical methods, such as those of nickel, copper, cobalt, and indium, (for example, by Kulesza et al. [4–10] and Cataldi et al. [11–15]), including the properties of hybrid hexacyanoferrates such as nickel–palladium [9] and ruthenium–cobalt [15].

A number of transition metal hexacyanoferrates are becoming widely used redox mediators for biosensors [1–2]. The possibility for selective detection of H_2O_2, produced by enzymatic glucose reaction with glucose oxidase, by its reduction on PB-modified electrodes was first demonstrated by Karyakin et al. [16], and later has been used for the development of sensors and biosensors due to its ability to decrease the kinetic barrier for reduction or oxidation of hydrogen peroxide [17–20]. Besides PB, other metal hexacyanoferrates investigated for hydrogen peroxide detection and in oxidase-based biosensors are CuHCF [21–23], cobalt hexacyanoferrate (CoHCF) [24–27], and nickel hexacyanoferrate (NiHCF) [28–30]. An important possible advantage is their increased stability over a wider pH range, particularly in alkaline solution. Electrocatalytic reactions of other species besides hydrogen peroxide have also been demonstrated on hexacyanoferrate films, for example of neurotransmitters [31] or thiosulphate at CoHCF films [32] and ascorbic acid at CuHCF films [33].

In this work, CoHCF and CuHCF films have been formed on carbon film electrodes. These carbon film electrodes, made from carbon film electrical resistors [34], have been shown to have a wide potential window, particularly after electrochemical conditioning, and possess advantageous properties for various applications such as trace metal electroanalytical sensors [35] and as substrates for oxidase-based biosen-

R. Pauliukaite · C. M. A. Brett (✉)
Departamento de Quimica, Universidade de Coimbra,
3004–535 Coimbra, Portugal
E-mail: brett@ci.uc.pt
Tel.: +351-239-835295
Fax: +351-239-835295

M. Florescu
Department of Physics,
Transilvania University of Brasov,
2200 Brasov, Romania

sors [26, 36]. They have recently been characterized by electrochemical impedance spectroscopy in various electrolytes over a wide pH range [37]. Hexacyanoferrate films are deposited on these carbon electrode substrates in three different ways: cycling of the electrode potential, galvanostatic and chemical deposition, electrochemical characterisation using cyclic voltammetry, and electrochemical impedance spectroscopy, and compared for the detection of hydrogen peroxide.

Experimental

Reagents

$CuCl_2 \cdot 2H_2O$, $CoCl_2 \cdot 6H_2O$, $K_3Fe(CN)_6$, and KCl were analytical grade and purchased from Merck (Germany). All solutions were prepared in Millipore Milli-Q nanopure water (resistivity ≥ 18 MΩ cm). Experiments were carried out at room temperature (24 ± 1°C).

Electrode preparation

The carbon film electrodes were made from carbon film electrical resistors (2 Ω resistance) [34, 35] of length 4 mm and diameter 1.5 mm. One of the gold contact caps is removed and the other with external contact wire is covered with a plastic sheath and epoxy resin, leaving an exposed electrode area of $\sim$0.20 cm^2 (Fig. 1). The films of CoHCF and CuHCF were deposited in three different ways:

- By potential cycling between 0.0 V and +0.9 V for CoHCF [27] or between +0.25 V and +0.9 V for CuHCF for 25 cycles at a scan rate of 50 mV s^{-1};
- By application of a constant current (-100 μA cm^{-2}) for 300 s;
- By direct adsorption, immersing the carbon film electrode substrate in the deposition solution.

All solutions for CoHCF film formation contained 100 mM KCl to which was added 1 mM $CoCl_2$ + 0.5 mM $K_3Fe(CN)_6$ for deposition by potential cycling; 5 mM $CoCl_2$ + 2.5 mM $K_3Fe(CN)_6$ for galvanostatic
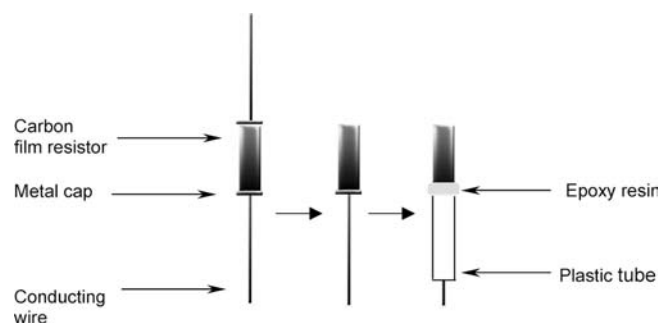

Fig. 1 Scheme of carbon film resistor electrode preparation

deposition, and 10 mM $CoCl_2$ + 10 mM $K_3Fe(CN)_6$ for chemical deposition. For CuHCF, the solution contained 10 mM $CuCl_2$, 10 mM $K_3Fe(CN)_6$, and 100 mM KCl for all three types of deposition.

After film formation, the electrodes were dried in a hot-air stream and left for 24 h in air to stabilize.

Instrumentation

Measurements were performed using a computer-controlled μ-Autolab Type II potentiostat/galvanostat with GPES 4.9 software (Eco Chemie, Netherlands). The three-electrode electrochemical cell contained the Co-HCF- or CuHCF-coated carbon film working electrode, a platinum foil counter electrode and a saturated calomel electrode (SCE) as reference.

Electrochemical impedance measurements were carried out in the same electrochemical cell with a PC-controlled Solartron 1250 frequency response analyser coupled to a Solartron 1286 electrochemical interface using ZPlot 2.4 software (Solartron Analytical, UK). A sinusoidal voltage perturbation of rms amplitude 10 mV was applied, scanning from 65 kHz to 0.1 Hz with ten points per frequency decade, integration time 120 s. Fitting to equivalent circuits was performed with ZView 2.4 software.

Results and discussion

Deposition of CoHCF and CuHCF films

Potential cycling

The most common method for deposition of metal hexacyanoferrates is cycling the potential applied to the electrode in appropriate electrolyte solutions [1–3]. Figure 2a shows deposition of CoHCF and CuHCF by potential cycling; the film growth depends on the ratio of the precursor salts and the hexacyanoferrate salt employed. From the variation of oxidation peak current with cycle number, it can be seen that the CoHCF film grows at a fast, constant rate up to 20 cycles and then more slowly (Fig. 2a1). A very small redox couple at +0.2 V disappeared completely after 15 cycles and the second at +0.4 V ($Co^{II} \leftrightarrow Co^{III}$) increased rapidly in size. A similar film growth on wax-impregnated graphite was reported in [38], using a slightly different deposition solution (0.5 M KCl rather than 0.1 M KCl).

Deposition of CuHCF by potential cycling shows a different behaviour to CoHCF. Fast growth occurred for only 5 cycles; the deposition rate then slowed down significantly and after 10 cycles, only insignificant changes occurred (Fig. 2a2). During CuHCF deposition, peaks corresponding to both redox couples, $Cu^{I} \leftrightarrow Cu^{II}$ and $Fe^{II} \leftrightarrow Fe^{III}$, are clearly seen.
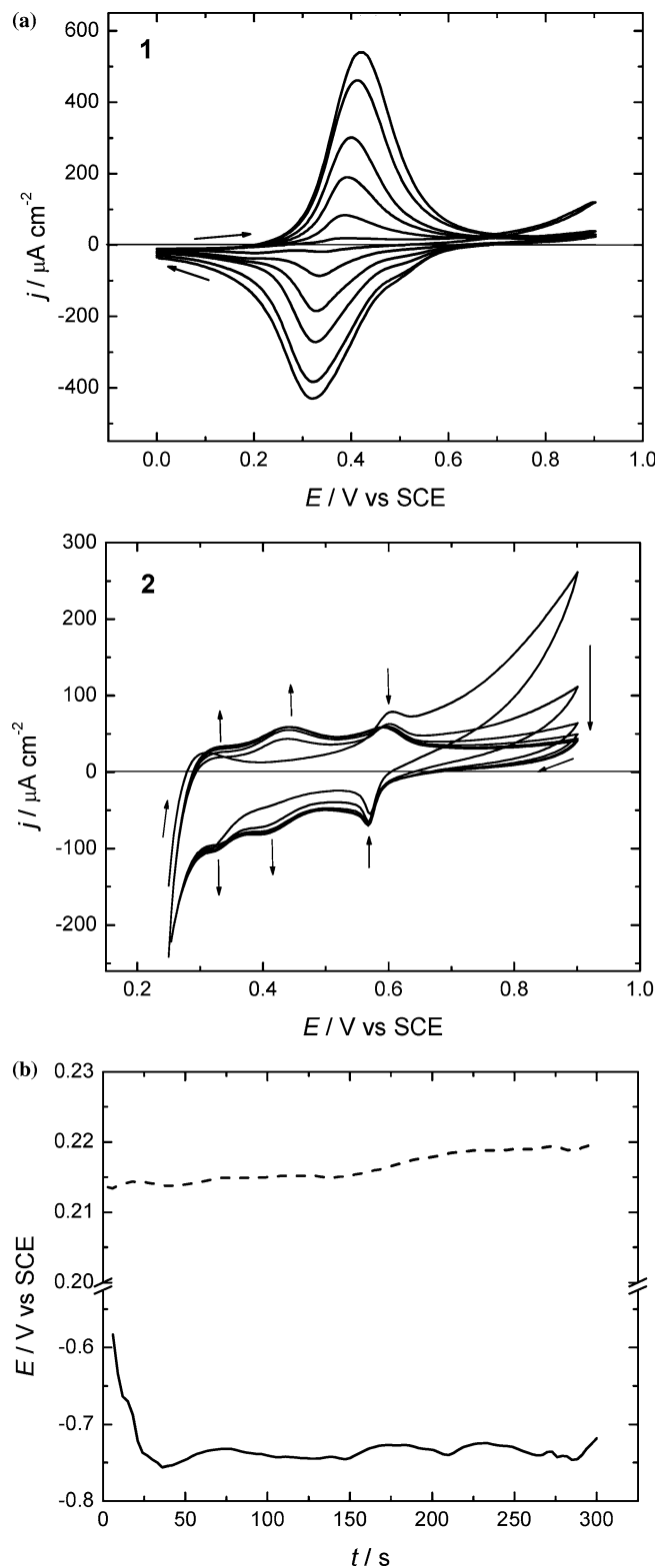
Fig. 2 **a** Cyclic voltammograms showing deposition of *1* CoHCF and *2* CuHCF by potential cycling — cycles 1, 5, 10, 15, 20, and 25. **b** Variation of potential with time during galvanostatic deposition of (———) CoHCF and (– – –) CuHCF

Galvanostatic deposition

A slightly different film growth was obtained by galvanostatic deposition. In the case of CoHCF, the potential decreased rapidly up to 30 s, then remained constant (Fig. 2b, solid line). During galvanostatic deposition of CuHCF, the potential slowly increased for the whole 300 s (Fig. 2b, dashed line). Although the same current (-100 mA cm^{-2}) was applied for both hexacyanoferrates, CoHCF and CuHCF, the deposition potential differed substantially, i.e. it was $\sim +0.22$ V versus SCE in the case of CuHCF, where usually Cu^{2+} reduction takes place, and in the case of CoHCF, it was much more negative ($\sim$-0.75 V versus SCE).

Two-step deposition methods have also been described. Usually a constant current is used in the first step to cause galvanostatic deposition of metal and then potential cycling is done in potassium hexacyanoferrate solution, e.g. [21]. It is also possible that here, during galvanostatic deposition from the metal hexacyanoferrate solution, the deposition occurs in two steps, i.e. first metal is deposited and then the fresh film reacts with $[Fe(CN)_6]^{3-}$. Nevertheless, there is no direct evidence of this.

Chemical immersion

Films were also deposited chemically by immersion of the carbon film electrodes in the deposition solution (details in Experimental section). A two-step chemical deposition has also been reported in this case, where metal was deposited by electroless plating and after this the electrode was immersed for a very short time in $K_3Fe(CN)_6$ solution [26].

Electrochemical characterisation of cobalt and copper hexacyanoferrates

Cyclic voltammetry

In general, films obtained by different methods have different structure and thickness [1]. On carbon film substrates, this is clearly seen in Fig. 3, which shows the electrochemical behaviour of the films in 0.1 M KCl solution after aging for one day at room temperature in air. The thickest films of both hexacyanoferrates were obtained by chemical deposition; chemical deposition is usually done for a longer time than the electrochemical procedures. Electrochemically deposited films also differ depending on whether potential cycling or application of a constant current is used: those obtained by potential cycling exhibited CVs quite different from those obtained galvanostatically, which were more similar to chemically deposited metal hexacyanoferrates. The charge under the cyclic voltammogram anodic peaks is $\sim$50 μC cm^{-2} for chemical deposition and galvanostatically formed films, and $\sim$5 μC cm^{-2} for films formed by potential cycling for other CoHCF and CuHCF films.
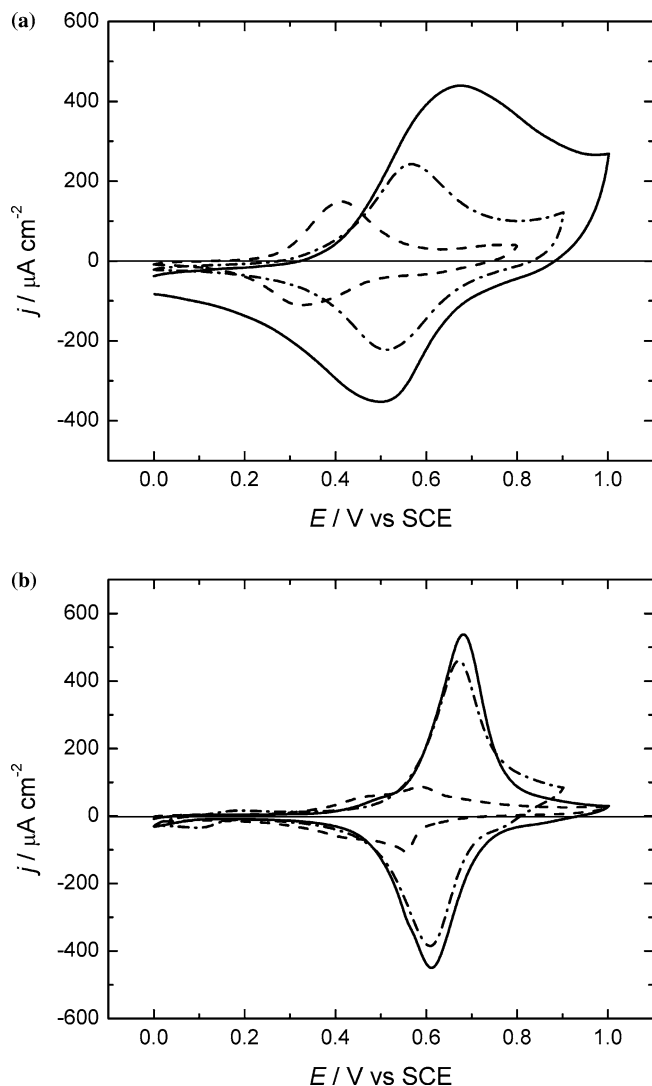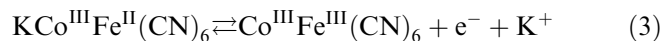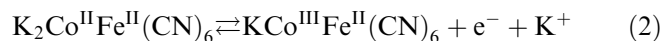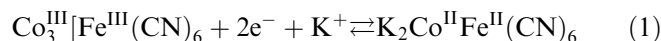
Fig. 3 Cyclic voltammograms in 0.1 M KCl of (**a**) CoHCF and (**b**) CuHCF films obtained by (– – –) potential cycling, (– · – · –) galvanostatically, and (———) chemically after 1 day of stabilization in air at room temperature. Potential sweep rate 50 mV s^{-1}

The CoHCF deposited chemically exhibits one redox couple with a quite large peak separation (Fig. 3a). This couple can probably be attributed to the summation of both processes $Co^{II} \leftrightarrow Co^{III}$ and $Fe^{II} \leftrightarrow Fe^{III}$. The redox couple is irreversible with a peak separation of 0.149 V for a chemically deposited CoHCF film. The reversible redox peaks on the galvanostatically deposited film are much smaller than on the chemically deposited film, with a peak separation of 0.05 V. Films deposited by potential cycling show two redox couples. The first of these, at less positive potentials than on chemically or galvanostatically prepared films, i.e. +0.3 V to +0.4 V, is due to $Co^{II} \leftrightarrow Co^{III}$, and the second (a small peak) at +0.6 V to +0.7 V versus SCE can be attributed to iron in the hexacyanoferrate ion [3, 39]. Thus, the structure of the CoHCF films changes according to the deposition method. A detailed study of CoHCF films deposited by potential cycling was done in a previous work [27].

A similar tendency was found with CuHCF films, except that the peaks are better defined than at CoHCF and the peak separation is smaller (Fig. 3b). The redox couple of the hexacyanoferrate anion is clearly seen at ~+0.6 V, and also $Cu^I \leftrightarrow Cu^{II}$ at +0.1–+0.15 V versus SCE [40] is visible at the galvanostatically deposited film, while at chemically deposited CuHCF, the first couple is suppressed and hardly evident. In the case of deposition by potential cycling, the peaks are closer to each other: the $Cu^{I/II}$ redox peaks are more positive (~+0.45 V) and $Fe^{II/III}$ peaks (~+0.57 V) are less positive than at galvanostatically deposited CuHCF films.
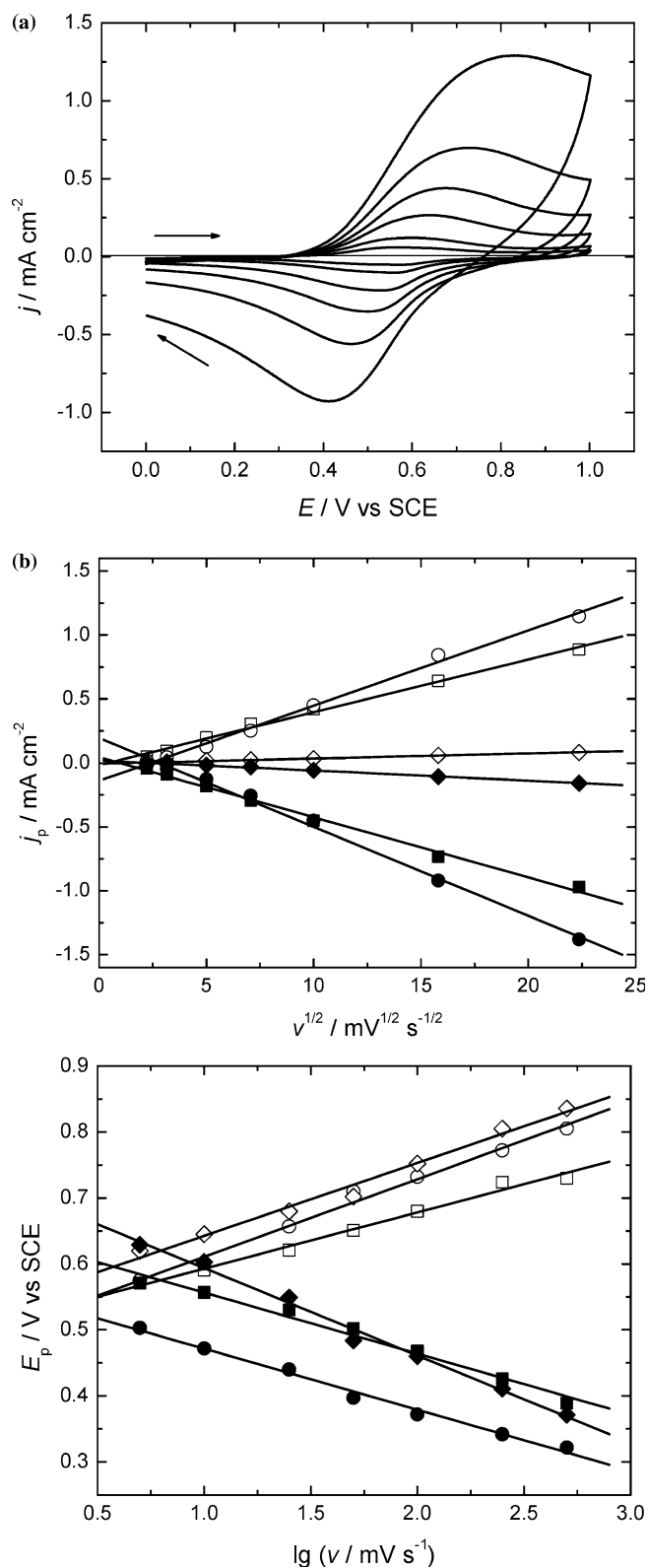
Figure 4 presents the analysis of CoHCF films in 0.1 M KCl by cyclic voltammetry at different potential sweep rates, v. Figure 4a shows CVs at CoHCF deposited chemically. At low sweep rates, 5 mV s^{-1} and 10 mV s^{-1}, double redox peaks are seen — oxidation at +0.6 V to +0.7 V and reduction at +0.5 V to +6 V versus SCE — which transform to one broad peak at faster sweep rates. The peak current shows a linear dependence on $v^{1/2}$ with slope ~±0.045 mA cm^{-2} mV$^{-1/2}$ s$^{1/2}$ (Fig. 4b, squares, Table 1), and $j_{p,a}/j_{p,c}$ is nearly 1 so that the electrochemical process at this film is close to being diffusion controlled. However, the peak position changes with increasing scan rate and peak separation increases. The dependence of the peak potential on lg v is linear with slope 0.085 for oxidation and −0.093 V/decade for reduction (Fig. 4b, squares).

These results suggest that the rate-determining step of the process could be diffusion of the cation of the supporting electrolyte for charge compensation during the electrochemical redox reaction of hexacyanoferrate(II/III) [39], such as given in the following scheme [25]:

$$Co_3^{III}[Fe^{III}(CN)_6 + 2e^- + K^+ \rightleftarrows K_2Co^{II}Fe^{II}(CN)_6 \quad (1)$$

$$K_2Co^{II}Fe^{II}(CN)_6 \rightleftarrows KCo^{III}Fe^{II}(CN)_6 + e^- + K^+ \quad (2)$$

$$KCo^{III}Fe^{II}(CN)_6 \rightleftarrows Co^{III}Fe^{III}(CN)_6 + e^- + K^+ \quad (3)$$

A similar peak dependence was found at CoHCF deposited by potential cycling, except in this case, the slope of the linear peak current dependence on $v^{1/2}$, ~0.004 mA cm^{-2} mV$^{-1/2}$ s$^{1/2}$ and ~−0.008 mA cm^{-2} mV$^{-1/2}$ s$^{1/2}$ (Fig. 4b, diamonds), for oxidation and reduction respectively, was much smaller than at the same film deposited by chemical immersion. These data are different from those obtained in [27] due to different experimental conditions. The peak potential dependence on lg v was similar to chemical CoHCF film with a slope of ~±0.12 V per decade.

A linear peak current dependence on square root of sweep rate was also found at galvanostatically deposited CoHCF films (Fig. 4b, circles); the slopes were 0.059 mA cm^{-2} mV$^{-1/2}$ s$^{1/2}$ and −0.07 mA cm^{-2} mV$^{-1/2}$ s$^{1/2}$. The change in peak position with scan rate is similar to that at chemically deposited CoHCF, with a linear dependence on lg v for both oxidation and reduction peaks. The slope of the oxidation plot is two

358

(a)

(b)

Fig. 4 Analysis of CoHCF films by cyclic voltammetry in 0.1 M KCl. **a** Cyclic voltammograms of CoHCF, deposited chemically, at sweep rates, v: 5 mV s^{-1}, 10 mV s^{-1}, 25 mV s^{-1}, 50 mV s^{-1}, 100 mV s^{-1}, 250 mV s^{-1}, and 500 mV s^{-1}. **b** Analysis of cyclic voltammograms of CoHCF deposited chemically (*open square, filled square*), galvanosta-tically (*open circle, filled circle*), and by potential cycling (*open diamond, filled diamond*): dependence of peak current, I_p, on $v^{1/2}$ and peak potential, E_p, on lg v

(Fig. 5). Figure 5a shows CVs at chemically deposited CuHCF at different scan rates. At low potential sweep rates (up to 10 mV s^{-1}), two redox peak couples are seen, the first broad and the second well defined; the first peak is suppressed at higher potential sweep rates.

The dependence of peak current on $v^{1/2}$ is linear at all CuHCF films studied (Fig. 4b) and the ratio between oxidation and reduction currents is close to 1 (Table 1). Both types of electrochemically deposited film show quite similar peak currents and slopes, while at chemically deposited CuHCF, the peak current is several times higher due to the thicker film. However, the peak potential dependence on lg v is not linear on any of the CuHCF films studied. This could be related to a different charge transfer mechanism to the film, since charge propagation is limited to counter ion transport [6, 39]. Also, CuHCF may have a different structure from Co-HCF films. There is evidence for this from previous work: Chen and Chan used the electrochemical quartz crystal microbalance to examine the oxidation state of Cu and Fe in CuHCF and, regarding copper, found that only Cu^{II} exists in the complex [39]. The same result was found analysing the CuHCF precipitate chemically [42] or by elemental analysis of CuHCF powder obtained chemically or by a coagulation procedure [43]. In the last case, it was found that CuHCF powder consists of a mixture of K$_{1.1}$Cu$_{1.15}$[Fe^{III}(CN)$_6$] and K$_{0.8}$Cu$_{1.6}$[Fe^{II}(CN)$_6$].

Electrochemical impedance spectroscopy

Further studies of the CoHCF and CuHCF films were carried out by electrochemical impedance spectroscopy (EIS). Spectra recorded at 0.0 V and +0.55 V versus SCE at the various films show some differences between the different deposition methods (Figs.6-7). A potential of 0.0 V was chosen because hydrogen peroxide oxidation

times higher than that of reduction (0.118 V/lg mV s^{-1} and −0.060 V/lg mV s^{-1} respectively).

A similar variation in electrochemical behaviour was also found in CuHCF films deposited in various ways

Table 1 Slopes of the peak current, j_p, versus square root of sweep rate, v, plots from CVs recorded in 0.1 M KCl solution at CoHCF and CuHCF films deposited in different ways

Hexacyano-ferrate	Film deposition method	Slope of j_p versus $v^{1/2}$/ mA cm^{-2} mV$^{-1/2}$ s$^{1/2}$	
		Oxidation peak	Reduction peak
CoHCF	Chemical	0.043	−0.047
CuHCF	Chemical	0.129	−0.117
	Galvanostatic	0.034	−0.033
	Potential cycling	0.024	−0.028

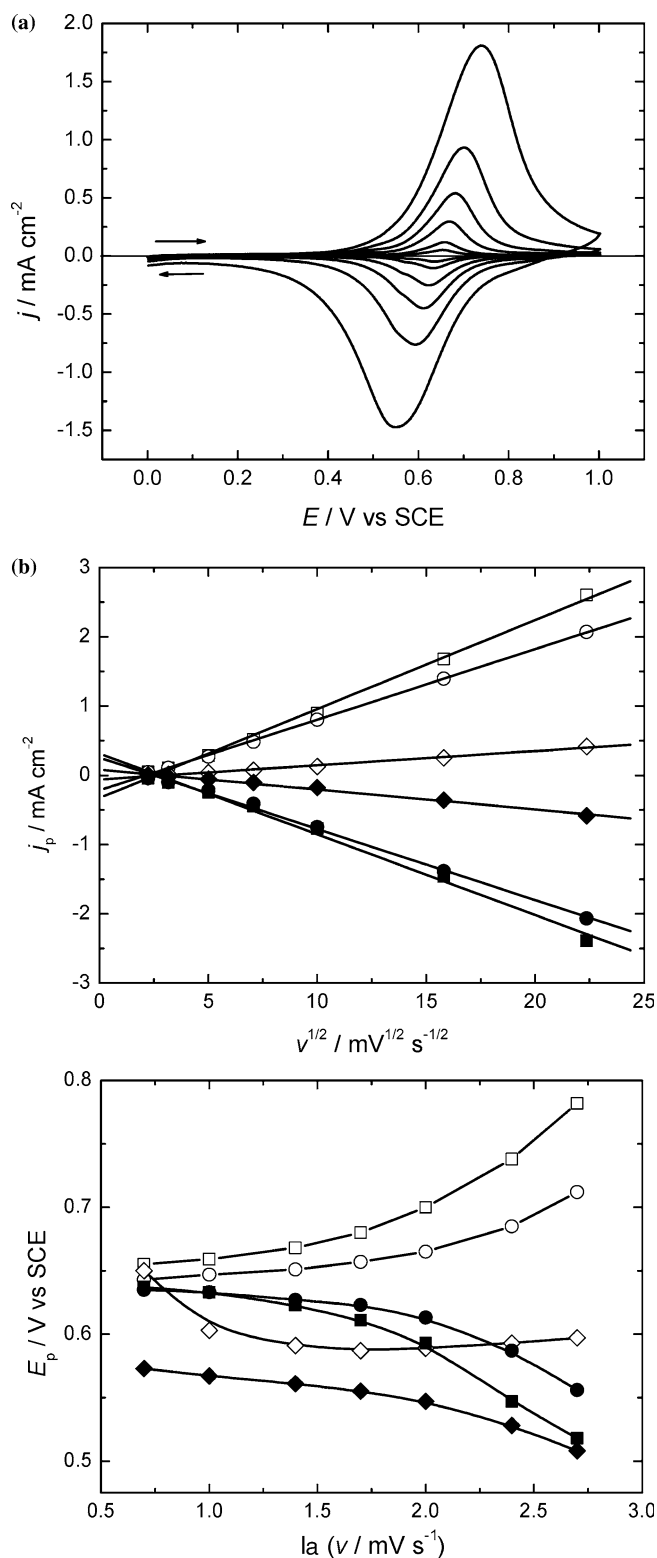Note: quantity calculus has been used.

Fig. 5 Analysis of CuHCF films by cyclic voltammetry in 0.1 M KCl. **a** Cyclic voltammograms of CuHCF, deposited chemically, at sweep rates, v: 5 mV s^{-1}, 10 mV s^{-1}, 25 mV s^{-1}, 50 mV s^{-1}, 100 mV s^{-1}, 250 mV s^{-1}, and 500 mV s^{-1}. **b** Analysis of cyclic voltammograms of CuHCF deposited chemically (*open square*, *filled square*), galvanosta-tically (*open circle*, *filled circle*), and by potential cycling (*open diamond*, *filled diamond*): dependence of peak current, I_p, on $v^{1/2}$ and peak potential, E_p, on lg v

was performed at this potential (see below), and the second of +0.55 V is where the film redox reaction takes place.

At 0.0 V (Fig. 6), both types of electrochemically deposited hexacyanoferrate films had similar impedance values (lower values in the case of galvanostatic deposition), while those from chemically deposited CoHCF and CuHCF films were higher, suggesting a more defect-free structure. These data are in agreement with cyclic voltammetry at these films. However, the results were different at +0.55 V (Fig. 7): the lowest impedance values were obtained at the films deposited chemically. The impedance spectra show charge transfer control at high frequencies and diffusion control represented as a finite-length open-terminus Warburg element at low frequencies, as in [44]. The frequency range of each zone depended on the nature of the hexacyanoferrate and film deposition method. Data obtained are in good agreement with those reported in the literature [44, 45].

For spectra obtained at 0.0 V versus SCE, modelling was done using a R_{ct}-CPE_1 parallel combination equivalent circuit in series with the cell resistance R_Ω, with R_{ct} representing the charge transfer resistance and CPE_1 a non-ideal capacitor of exponent n_1 for fitting the spectra at 0.0 V (Fig. 6c), and the circuit was extended with a finite-length open terminus Warburg element in series at +0.55 V, as in [44], to represent cation diffusion in the metal hexacyanoferrate film (Fig 7c). The values of the fitted parameters are presented in Table 2, where C_1 and n_1 are calculated for CPE_1 and C_2 and n_2 for the open-terminus Warburg element, W_o. They clearly show that both chemically deposited films have similar properties, but electrochemically deposited ones are slightly different, which suggests different structures obtained by chemical and electrochemical deposition.

Impedance studies at thin and thick CoHCF films at open circuit potential were reported in [3], where the thicker film showed a larger resistance and capacitance relaxation. However, impedance spectra depended not only on the thickness of the film, but also on the nature of counter cation. In other works and in order to calculate the diffusion coefficients of electrons and K$^+$ in the CuHCF composite (a mixture of CuHCF and graphite powder), impedance spectra were also recorded at +0.64 V, +0.69 V, and +0.74 V versus Ag/AgCl (where the redox process of CuHCF takes place) in 0.1 M KNO$_3$ [44]. Impedance spectra at those potentials had two regions, as found here by us: a semi-circle at high frequencies and finite-length open-terminus Warburg/capacitive region at low ones, and the frequency range depended on the nature of CuHCF [44, 45].

Response to hydrogen peroxide

All films were tested for the determination of hydrogen peroxide in 0.1 M phosphate buffer saline (PBS) solution, pH 7, at 0.0 V versus SCE in order to find the best ones for application in oxidase enzyme biosensors. The

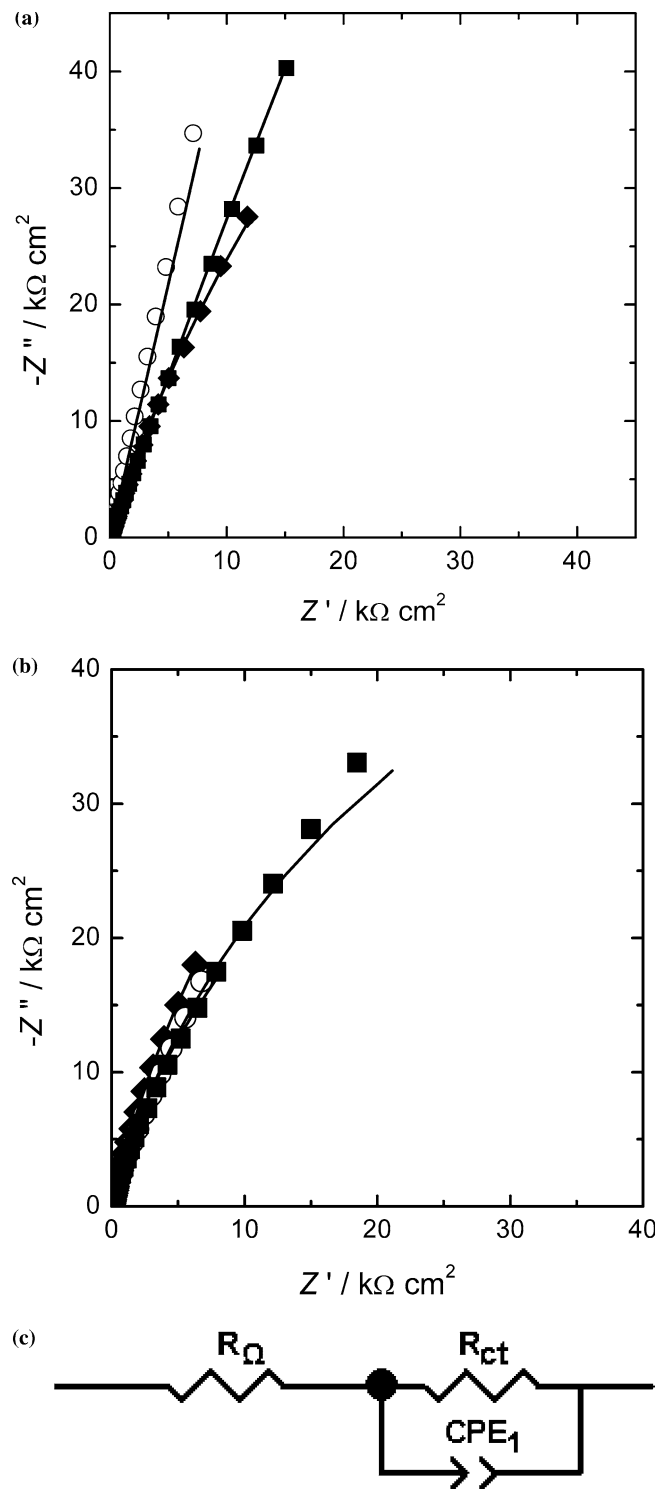films were first characterized by cyclic voltammetry in 0.1 M PBS electrolyte, pH 7. The CVs (not shown) are similar to those obtained in KCl solution, except that the peaks are not so well defined and are shifted ~0.1 V to more positive potentials. The CoHCF and CuHCF peaks decrease in height with the addition of H_2O_2 analyte, the extent depending on the way the film was deposited. Films of both hexacyanoferrates deposited at
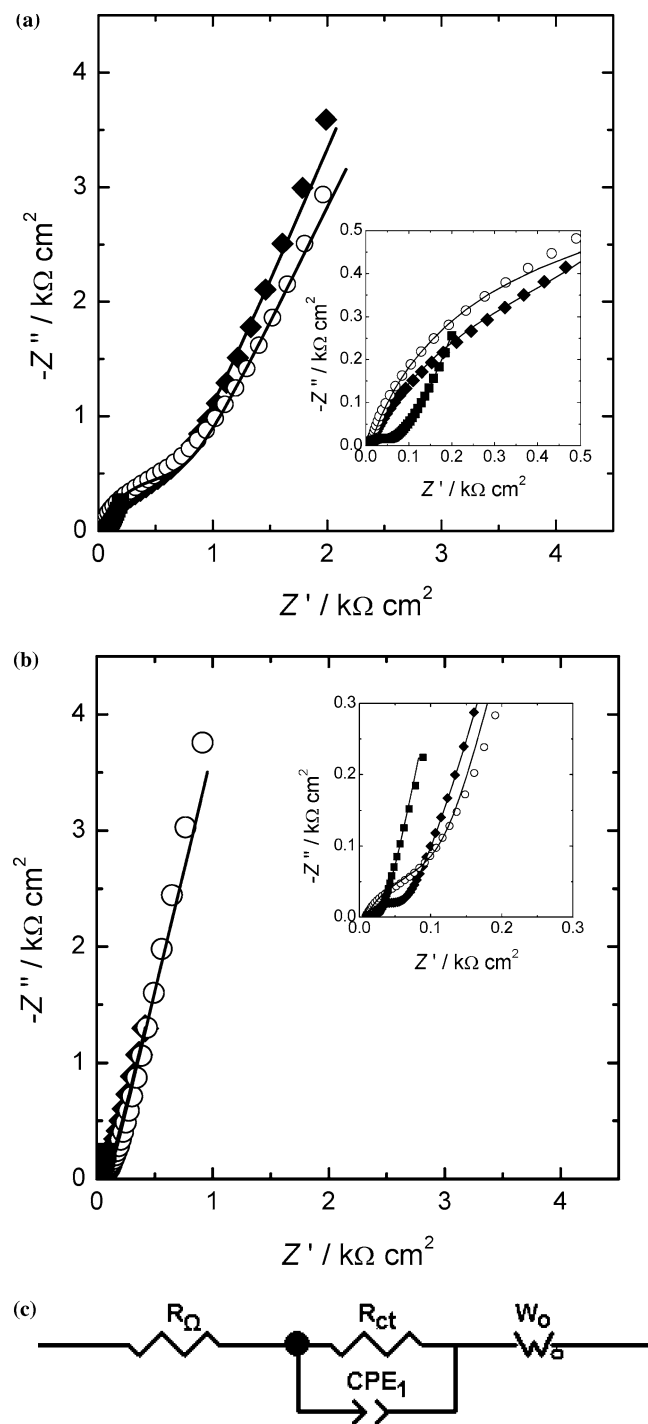

Fig. 6 Complex plane impedance spectra at 0.0 V of (**a**) CoHCF and (**b**) CuHCF deposited chemically (*filled square*), galvanostatically (*open circle*), and voltammetrically (*filled diamond*): *symbols* indicate the experimental data and lines the fitting using the equivalent circuit shown in (**c**). Supporting electrolyte 0.1 M KCl

Fig. 7 Complex plane impedance spectra at 0.55 V of (**a**) CoHCF and (**b**) CuHCF deposited chemically (*filled square*), galvanostatically (*open circle*), and voltammetrically (*filled diamond*): *symbols* indicate the experimental data and lines the fitting using the equivalent circuit shown in (**c**). Supporting electrolyte 0.1 M KCl

Table 2 Calculated parameters from electrochemical impedance spectra (Figs. 6 and 7)

E/V versus SCE	Film	R_Ω/kΩ cm^{-2}	R_{ct}/ kΩ cm^2	C_1/μF cm^{-2} s$^{n_1-1}$	n_1	C_2/μF cm^{-2} s$^{n_2-1}$	n_2
0.0	CoHCF (chemical)	15.4	2165	33.0	0.79	–	–
	CoHCF (galvanostatic)	10.3	–	42.4	0.86	–	–
	CoHCF (voltammetry)	9.3	243	45.5	0.81	–	–
	CuHCF (chemical)	7.9	118	32.1	0.84	–	–
	CuHCF (galvanostatic)	7.8	95	73.2	0.85	–	–
	CuHCF (voltammetry)	7.5	156	74.4	0.86	–	–
0.55	CoHCF (chemical)	7.6	0.03	66.0	0.82	7.69	0.46
	CoHCF (galvanostatic)	9.4	0.62	68.7	0.85	0.01	0.45
	CoHCF (voltammetry)	8.2	0.60	108	0.75	0.34	0.42
	CuHCF (chemical)	2.5	0.003	12.6	0.92	6.71	0.48
	CuHCF (galvanostatic)	8.8	0.11	91.4	0.80	0.04	0.43
	CuHCF (voltammetry)	7.9	0.04	69.9	0.78	1.20	0.47

Note: Quantity calculus has been used.

constant current exhibited the least decrease with increase in hydrogen peroxide concentration. The highest decrease of the peak current was at CuHCF deposited by chemical adsorption. The results led us to conclude that, at this pH, electrocatalytic reduction of hydrogen peroxide occurs with the formation of hydroxyl ions:

$$H_2O_2 + 2e \rightarrow 2OH^- \qquad (4)$$

The product of the electrocatalytic reduction causes a decrease in the height of the CoHCF and CuHCF peaks. A similar behaviour was found in a previous work with PB films [46].

The amperometric response to hydrogen peroxide at CoHCF deposited by potential cycling has been described previously [27]: the sensitivity was 17.2 nA μM^{-1}, with a very low detection limit of 0.27 μM, and the linear range was up to 5 μM.

The response to hydrogen peroxide at CoHCF and CuHCF films deposited in different ways is shown in Fig. 8, excluding CoHCF formed by potential cycling since the available concentration range is not easily seen on this scale. CoHCF deposited at constant current gave a poor response; chemical deposition led to a linear response over the whole concentration range studied, but sensitivity was not better than at the voltammetrically deposited film. Moreover, CoHCF films showed some lack of stability at neutral pH, although it has been reported that CoHCF, formed at PB electrodes by cycling the potential in CoCl$_2$ solution, had a much better stability at neutral pH than the PB electrode [47]. However, it is possible that the authors obtained a mixed cation hexacyanoferrate, which are known to be more stable than those containing monocations [13, 48, 49].

CuHCF films deposited by potential cycling had a better sensitivity than CoHCF deposited chemically, but the linear range is not large enough for a biosensor. CuHCF deposited galvanostatically gave a poor response, similar to CuHCF deposited by potential cycling.

The best analytical properties from the films studied were from CuHCF deposited chemically with a sensi-

tivity of 1.11 nA μM^{-1}, a linear range from 10 to 600 μM, and detection limit 2.1 μM. Although it did not have as high a sensitivity and low limit of detection as the CoHCF studied in [27], it had a longer linear range and suitable sensitivity to be applied for electrochemical biosensors. Moreover, it was the most stable film of those described. A high stability at neutral pH (pH 7.3) for the determination of H$_2$O$_2$ was also reported in [21], where CuHCF was deposited in 2 steps: galvanostatic pre-deposition of Cu and then cycling in hexacyanoferrate solution, operating at −0.2 or 0.0 V Ag/AgCl.

All other films showed a lower sensitivity to hydrogen peroxide than CuHCF deposited chemically: CoHCF deposited by chemical immersion had a sensitivity 0.18 μM nA^{-1}, linear range up to 1 mM, and detection limit 5.3 μM; CuHCF deposited by potential cycling had better sensitivity than CoHCF deposited by immersion, i.e. 0.86 nA μM^{-1}, and similar detection limit 5.0 μM but the linear range was much shorter, i.e. up to
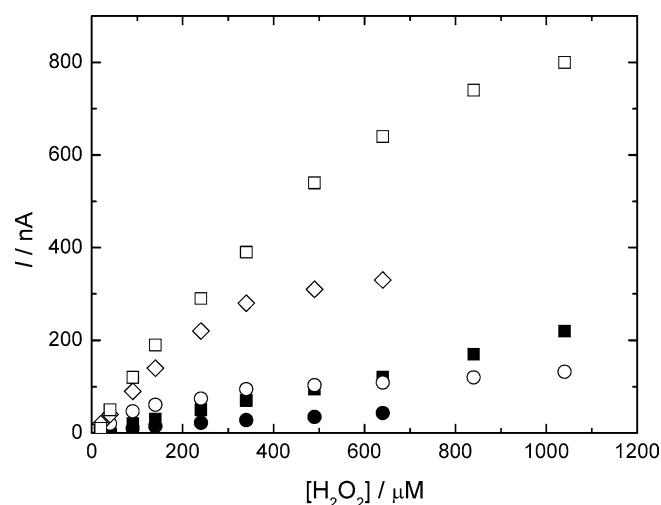
Fig. 8 Response to hydrogen peroxide at +0.05 V versus SCE in 0.1 M PBS at CoHCF (*black symbols*) and CuHCF (*white symbols*) deposited chemically (*filled square, open square*), galvanostatically (*filled circle, open circle*), and voltammetrically (*open diamond*)

350 μM. Galvanostatically deposited films had a poor sensitivity to H_2O_2.

Conclusions

Copper hexacyanoferrate and CuHCF, deposited at carbon film resistor electrodes by three different one-step processes, cycling of the electrode potential, by application of a constant current, or chemically, were characterized electrochemically using cyclic voltammetry and electrochemical impedance spectroscopy. Electrochemical redox reactions of the films were limited by diffusion of the counter cation. To evaluate the films for possible use as redox mediators for biosensors, they were applied to the determination of hydrogen peroxide in neutral media. Although CoHCF made by potential cycling is the most useful when a very low detection limit is necessary over a short timescale, chemically deposited CuHCF was found to be generally the most suitable as a mediator for biosensors.

References

1. Koncki R (2002) Crit Rev Anal Chem 32:79
2. Karyakin AA (2001) Electroanalysis 13:813
3. de Tacconi RN, Rajeshwar K, Lezna RO (2003) Chem Mater 15:3046
4. Horányi G, Inzelt G, Kulesza PJ (1990) Electrochim Acta 35:811
5. Kulesza PJ, Galus Z (1992) J Electroanal Chem 323:261
6. Kulesza PJ, Malik MA, Miecznikowski K, Wolkiewicz A, Zamponi S, Berrettoni M, Marassi R (1996) J Electrochem Soc 143:L10
7. Malik MA, Horányi G, Kulesza PJ, Inzelt G, Kertész V, Schmidt R, Czirok E (1998) J Electroanal Chem 452:57
8. Kulesza PJ, Malik MA, Berrettoni M, Giogetti M, Zamponi S, Schmidt R, Marassi R (1998) J Phys Chem B 102:1870
9. Kulesza PJ, Malik MA, Schmidt R, Smolinska A, Miecznikowski K, Zamponi S, Czerwinski A, Berrettoni M, Marassi R (2000) J Electroanal Chem 487:57
10. Malik MA, Miecznikowski K, Kulesza PJ (2000) Electrochim Acta 45:3777
11. Cataldi TRI, Centonze D, Guerrieri (1995) Anal Chem 67:101
12. Cataldi TRI, Guascito R, Salvi AM (1996) J Electroanal Chem 417:83
13. Cataldi TRI, De Benedetto GE, Bianchini A (1998) J Electroanal Chem 448:111
14. De Benedetto GE, Guascito MR, Ciriello R, Cataldi TRI (2000) Anal Chim Acta 410:143
15. Cataldi TRI, De Benedetto G, Bianchini A (1999) J Electroanal Chem 471:42
16. Karyakin AA, Gitelmacher OV, Karyakina EE (1994) Anal Lett 27:2861
17. Karyakin AA, Karyakina EE, Gorton L (1996) Talanta 43:1597
18. Chi QJ, Dong SJ (1995) Anal Chim Acta 310:429
19. Moscone D, D'Ottavi D, Compagnone D, Palleschi G, Amine A (2001) Anal Chem 73:2529
20. O'Halloran MP, Pravda M, Guilbault GG (2001) Talanta 55:605
21. Garjonyte R, Malinauskas A (1999) Sens Actuat B 56:93
22. Wang J, Zhang XJ, Prakash M (1999) Anal Chim Acta 395:11
23. Mattos IL, Gorton L, Laurell T, Malinauskas A, Karyakin AA (2000) Talanta 52:791
24. Lin MS, Wu YC, Jan BI (1999) Biotechnol Bioeng 62:56
25. Chen SM (2002) J Electroanal Chem 521:29
26. Eftekhari A (2003) Microchim Acta 141:15
27. Florescu M, Brett CMA (2004) Anal Lett 37:871
28. Cai CX, Xue KH, Zhou YM, Yang H (1997) Talanta 44:339
29. Milardović S, Kruhak I, Iveković D, Rumenjak V, Tkalčec M, Grabarić BS (1997) Anal Chim Acta 350:91
30. de Mattos IL, Gorton L (2001) Quim Nova 24:200
31. Chen S-M, Peng K-T (2003) J Electroanal Chem 547:179
32. Shankaran DR, Narayanan SS (2002) Sens Actuat B 86:180
33. Shankaran DR, Narayanan SS (1999) Fresen J Anal Chem 364:686
34. Brett CMA, Angnes L, Liess HD (2001) Electroanalysis 13:765
35. Filipe OMS, Brett CMA (2003) Talanta 61:643
36. Florescu M, Brett CMA (2005) Talanta 65:306
37. Filipe OMS, Brett CMA (2004) Electroanalysis 16:994
38. Joseph J, Gomathi H, Rao GP (1991) J Electroanal Chem 304:263
39. Chen SM, Chan CM (2003) J Electroanal Chem 543:161
40. Shankaran DR, Narayanan SS (1999) Fresen J Anal Chem 364:686
41. Lezna RO, Romangnoli R, de Tacconi NR, Rajeshwar K (2002) J Phys Chem B 106:3612
42. Antunes RMM, Sequeira CAC (2004) Ciênc Tecnol Mater (in Portuguese) 16:66
43. Makowski O, Stroka J, Kulesza PJ, Malik MA, Galus Z (2002) J Electroanal Chem 532:157
44. Kahlert H, Retter U, Lohse H, Siegler K, Scholz F (1998) J Phys Chem B 102:8757
45. Cardoso WS, Francisco MSP, Lucho AMS, Glushikem Y(2004) Solid State Ionics 167:165
46. Karyakin AA, Karyakina EE, Gorton L (1999) Electrochem Commun 1:78
47. Malinauskas A, Araminaitė R, Mickevičiūtė G, Garjonytė R (2004) Mat Sci Eng C 24:513
48. Dostal A, Hermes M, Scholz F (1996) J Electroanal Chem 415:133
49. Mo JW, Ogorevc B, Zhang X, Pihlar B (2000) Electroanalysis 12:48